# A Context Adaptive Bit-Plane Coder With Maximum-Likelihood-Based Stochastic Bit-Reshuffling Technique for Scalable Video Coding

Wen-Hsiao Peng, Tihao Chiang, *Senior Member, IEEE*, Hsueh-Ming Hang, *Fellow, IEEE*, and Chen-Yi Lee, *Member, IEEE*

***Abstract*—In this paper, we propose a context adaptive bit-plane coding (CABIC) with a stochastic bit reshuffling (SBR) scheme to deliver higher coding efficiency and better subjective quality for fine granular scalable (FGS) video coding. Traditional bit-plane coding in FGS algorithm suffers from poor coding efficiency and subjective quality. To improve coding efficiency, our CABIC constructs context models based on both the energy distribution in a block and the spatial correlations in the adjacent blocks. Moreover, it exploits the context across bit-planes to save side information. To improve subjective quality, our SBR reorders the coefficient bits by their estimated rate-distortion performance. Particularly, we model transform coefficients with Laplacian distributions and incorporate them into the context probability models for content-aware parameter estimation. Moreover, our SBR is implemented with a dynamic priority management that uses a low-complexity dynamic memory organization. Experimental results show that our CABIC improves the PSNR by 0.5$\sim$1.0 dB at medium and high bit rates. While maintaining similar or even higher coding efficiency, our SBR improves the subjective quality.**

***Index Terms*—Bit-plane coding, fine granularity scalability, scalable video coding.**

## I. Introduction

SCALABLE video coding attracts wide attention with the rapid growth of multimedia applications over Internet and wireless channels. In such applications, the video may be transmitted over error-prone channels with fluctuated bandwidth. To serve multimedia applications under a heterogeneous environment, MPEG-4 has defined the fine granularity scalability (FGS) [7] that provides a discrete cosine transform (DCT)-based scalable approach in a layered fashion. Currently, the base layer is coded by a non-scalable codec while the enhancement layer is coded with an embedded bit-plane coding using variable-length code (VLC). While offering FGS, current bit-plane coding poses two major disadvantages.

1) Poor coding efficiency: Poor coding efficiency is contributed by three factors. Firstly, information with different weighting is jointly grouped by (Run, EOP) symbols and coded without differentiation. Secondly, the coding of each bit-plane is independent and the coding of each DCT block is uncorrelated with adjacent neighbors. Existing correlations across bit-planes and among spatially adjacent blocks are not fully exploited. Lastly, the VLC tables have limitations to adapt the statistics for each sequence.
2) Poor subjective quality: Poor subjective quality is caused by the frame raster scanning. For each bit-plane, the current approach performs the coding in a block-by-block manner. As the enhancement layer is partially decoded, the frame raster scanning may only refine the upper part with one extra bit-plane. Such uneven refinement causes the degradation of subjective quality.

In this paper, our goal is to provide a generic bit-plane coding that delivers higher coding efficiency and better subjective quality. Our scheme is useful not only for MPEG-4 FGS [7], but also for the advanced FGS algorithms, [3], [4], [9], [12], [15].

For improving the coding efficiency, our prior work [10] has shown that simply replacing VLC with arithmetic coding is insufficient unless efficient context model are used. The existing approaches, [5], [8], have taken the context adaptive bit-plane coding (CABIC) for the DCT-based image coding. Specifically, the transform coefficients are first partitioned into significant bits and refinement bits, as in [13]. Then, the context model for each type of bits is designed according to different correlations. In [5], the energy distribution of $8 \times 8$ DCT is used to construct a "Run" index for the significant bit. In [8], the spatial correlations are considered by referring to the significance status of the adjacent and co-located coefficients as the context model. However, for predictive enhancement-layer coding in the advanced FGS algorithms, [3], [4], [9], [12], [15], using context models of lower order is insufficient because the signal is more like noise. To tackle this problem, our prior work [11] designs context models by jointly considering the energy distribution in a block and the spatial correlations in the adjacent blocks. Moreover, we employ the context across bit-planes to save side information. Although the context models are different, all the schemes try to fully use the existing correlations for better coding efficiency.

While the coding efficiency is improved by the CABIC, the poor subjective quality from the frame raster scanning still remains. For improving the subjective quality, MPEG-4 FGS [7] offers a frequency weighting tool. The basic idea is to shift up the coefficients of lower frequency so that they can be transmitted first. The subjective quality is improved since the refinement of each block becomes more uniform. However, the shift introduces

Manuscript received August 20, 2004; revised May 25, 2005. The associate editor coordinating the review of this manuscript and approving it for publication was Dr. Chang Wen Chen.

The authors are with the Department of Electronics Engineering, National Chiao-Tung University, Hsinchu 30010, Taiwan, R.O.C. (e-mail: pawn@mail.si2lab.org; tchiang@mail.nctu.edu.tw; hmhang@mail.nctu.edu.tw; cylee@cc.nctu.edu.tw).

Digital Object Identifier 10.1109/TMM.2006.876302

redundant bits that decrease the coding efficiency. On the average, at the same bit rate, a PSNR loss of 2∼3 dB is observed when the frequency weighting is enabled. To keep high coding efficiency, [1] presents a deterministic, group-based coding order. The transform coefficients in each block are partitioned into several subgroups. The coding of a subgroup can only be started when the previous subgroup of all blocks is finished. Apparently, the deterministic partition is not optimized for every sequence.

To adapt the coding order for different input sequences, dynamic bit-reshuffling schemes are proposed in our prior work [11] and the work by Li *et al.* [6]. The idea of bit reshuffling is to dynamically determine the coding order of each bit by its estimated rate-distortion performance. The coefficient bit with better rate-distortion performance is coded with higher priority. In [6], the bit reshuffling was first proposed to provide rate-distortion optimization specifically for the wavelet-based image codec. In [11], it is used to improve the subjective quality of the FGS algorithms. Previous results in [11] show that dynamic bit reshuffling can effectively improve the subjective quality while maintaining similar or even higher coding efficiency.

In this paper, we propose an enhanced stochastic bit-reshuffling (SBR) scheme. Instead of using the uniform distribution in [6], we model transform coefficients with discrete Laplacian distributions, which are derived from maximum likelihood principle. Moreover, we incorporate the context probability models into the discrete Laplacian distributions to estimate the rate-distortion functions of the transform coefficients. Furthermore, to make bit reshuffling content aware so as to improve the subjective quality, a dynamic priority management is developed by considering a content dependent priority and a rate-distortion data update mechanism. Since the bit reshuffling requires intensive computations, we further propose a dynamic memory organization to reduce complexity. In summary, our contributions and the features of this work include the following.

- A CABIC scheme that constructs context models based on both the energy distribution in a block and the spatial correlations in the adjacent blocks to deliver higher coding efficiency.
- A bit-plane partition scheme that exploits the context across bit-planes to save side information.
- An estimated Laplacian distribution is used for efficient coding of refinement bits.
- A maximum likelihood estimator is used to minimize the overhead for the Laplacian parameters.
- A $4 \times 4$ integer transform in [14] is used to avoid the context dilution problem.
- A content aware SBR that uses estimated Laplacian distributions and context probability models to improve subjective quality.
- A dynamic priority management implemented with a dynamic memory organization is used for SBR.

Experimental results show that our CABIC provides a PSNR gain of 0.5∼1.0 dB over the VLC-based bit-plane coding [7]. While maintaining similar or even higher coding efficiency, our SBR significantly improves the subjective quality.

The rest of this paper is organized as follows: Section II presents the algorithm of CABIC. Section III introduces the concept of SBR. Section IV shows the parameter estimation in SBR. Sections V and VI elaborate the dynamic priority management and memory organization. Section VII assesses the rate-distortion performance. Finally, Section VIII summarizes this work.

## II. Context Adaptive Bit-Plane Coding

In this section, we present a CABIC framework for coding the enhancement layer in FGS algorithms. Firstly, we introduce a context-adaptive binary arithmetic coder, which is incorporated in our CABIC as the entropy coder. Then, we present our bit classification and bit-plane partition schemes that are used for improving the efficiency of context utilization. Further, for each type of bits, we detail its context model. Lastly, we illustrate the coding flow of the proposed CABIC.

For the descriptions in the subsequent sections, we define our terminologies for the MSB bit and MSB bit-planes as follows: 1) the MSB bit represents the most significant bit of a coefficient; 2) the MSB bit-plane of a block denotes the one that includes the MSB bit of the maximum coefficient in a block; and 3) the MSB bit-plane of a frame is the one that contains the MSB bit of the maximum coefficient in a frame.

### A. Context-Adaptive Binary Arithmetic Coding

For better coding efficiency, our CABIC incorporates a context-adaptive binary arithmetic coder. The bit-planes are coded in a context-adaptive, bit-by-bit manner. As compared to VLC, context-adaptive binary arithmetic coding offers better capability of correlation utilization, statistical adaptation, and is closer to the entropy. Generally, its procedure includes the following 4 steps: 1) reference of context model; 2) retrieval of context probability; 3) binary arithmetic coding; and 4) update of probability model. Among these steps, the context reference is most critical to the coding efficiency.

### B. Bit Classification and Bit-Plane Partition

To improve the efficiency of context reference, we propose a bit-classification scheme and a bit-plane partition method for distinguishing the coefficient bits with different importance so that the context models can be designed by different sources of correlations. For the bit classification, we partition the coefficient bits into three types including significant bit, refinement bit and sign bit, as in [13]. Additionally, for each bit-plane of a transform block, we propose two side information symbols that are end-of-significant-bit-plane (EOSP) and Part_II_ALL_ZERO. The EOSP symbol is coded after a nonzero significant bit to notify the end of significant bit coding and the Part_II_ALL_Zero symbol is used to represent a group of zero significant bits.

For higher coding efficiency, a bit-plane partition method is further employed to save EOSP bits. We observe that the magnitude of a high-frequency coefficient is generally smaller than that of a low-frequency one. When the coding is conducted from the MSB bit-plane to the LSB bit-plane, such energy distribution suggests that the last nonzero significant bit of a bit-plane is more probable to appear after the one of the previously coded bit-plane in zigzag order. According to this observation, we partition the significant bits of each bit-plane into two parts. From the location of last nonzero significant bit in the previously coded

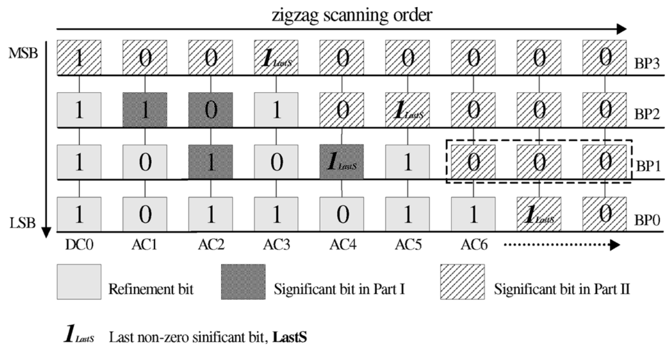


Fig. 1. Examples of bit classification and bit-plane partition in a transform block.

TABLE I
PROBABILITY FOR THE EOSP OF A BIT-PLANE BEING IN PART I

| Bit-plane | Mobile (CIF) | Stefan (CIF) |
|---|---|---|
| 5 (MSB) | 0.00* | 0.00* |
| 4 | 0.06 | 0.10 |
| 3 | 0.10 | 0.07 |
| 2 | 0.19 | 0.07 |
| 1 | 0.37 | 0.15 |
| 0 (LSB) | 0.55 | 0.32 |

*: All the significant bits in the MSB bit-plane are considered as Part II.

bit-plane, named LastS, Part I refers to the significant bits before LastS and Part II covers the remaining significant bits. Since the last nonzero significant bit of a bit-plane, i.e., the actual EOSP, probably locates in Part II, we can save EOSP bits by coding them only after the nonzero significant bits in Part II. Fig. 1 depicts a practical example, where each column denotes the binary representation of a coefficient and each row represents a bit-plane. For the bit-plane partition, we note that the LastS of BP3 is at AC3. Thus, in BP2, the significant bits before AC3 are classified as Part I and the remaining ones are classified as Part II. In this example, we save the EOSP bit that should be coded after the nonzero significant bit of AC1 and at BP2. By applying our partition scheme to each bit-plane, more EOSP bits can be saved.

Although the bit-plane partition saves EOSP bits, the missed prediction of EOSP location could introduce considerable overhead. Since we predict that the actual EOSP of a bit-plane locates in Part II, the coding is expected to stop somewhere in Part II. When the missed prediction occurs, the redundant zero significant bits after the actual EOSP will be coded. An example is shown in Fig. 1, where the LastS of BP1 is before the LastS of BP2. Thus, the redundant zero significant bits grouped by the dash rectangle at BP1 will be coded. In Table I, we analyze the probability that the EOSP actually locates in Part I. As shown, the missed prediction is below 10% in the higher bit-planes while it is about 32%–50% in the lower bit-planes. To address the missed prediction, a Part_II_ALL_ZERO symbol is encoded prior to the coding of the significant bits in Part II for notifying the all zero case.

### C. Design of Context Model

With our bit classification and bit-plane partition, this section further presents our context model for each type of bits. Particularly, we may jointly consider multiple factors as a context model.

*1) MSB_REACHED:* The MSB_REACHED symbol is a side information bit that indicates whether the MSB bit-plane of a block is reached. Approximately, the MSB_REACHED status of a block reveals the maximum energy in a block. Since adjacent blocks generally have similar energy distribution, we refer to the MSB_REACHED status of the nearest four blocks as context model. Specifically, we take the summation of the MSB_REACHED status in the nearest four blocks as context index.

*2) Significant Bit:* From the MSB bit-plane to the LSB bit-plane of a block, the significant bits of a coefficient are those before (and include) its MSB bit. During the bit-plane coding, we use significance status to represent the significant bits for a coefficient. Such status is initialized with zero and updated to the one when the MSB bit is coded. Statistical analysis shows that significant bits make up 80%–97% of the coefficient bits in the higher (MSB) bit-planes while they still represent 33%–51% in the lower (LSB) bit-planes. Therefore, the coding efficiency of significant bits is critical to the overall coding performance.

For efficiently coding significant bits, we jointly consider multiple factors as context model. We observe that 1) the nonzero coefficients with similar magnitude typically appear and cluster in zigzag scanning path; 2) the co-located coefficients in the spatially adjacent transform blocks have similar magnitude; and 3) the correlation varies with the frequency band. During the bit-plane coding, the significance status approximately reveals the magnitude of a coefficient. Thus, through the significance status, we map our observations into meaningful context model in Table II. For better understanding, Fig. 2 depicts an example of our context model for the significant bit. According to Table II, we can tell that the "Run" index is 1, the "Sum of Significance Status" is 3, and the "Frequency Band" is 8.

*3) Refinement Bit:* The refinement bit represents less predictable information. Statistical analysis shows that the refinement bits in the lower bit-planes may make up 50% or more. Thus, the coding efficiency of refinement bits is critical to the rate-distortion performance at high bit rates. Instead of using a fixed context probability model for all the refinement bits [5], [8], we use an estimated Laplacian model to derive the coding probability for each refinement bit. There is no context model specifically designed for the refinement bit. In Section IV, we use an example to illustrate how to calculate the coding probability for a refinement bit.

*4) Sign Bit:* The sign bit records the sign of a coefficient. Statistical analysis reveals that the distribution of a transform coefficient is approximately symmetric with respect to zero, i.e., the sign bit averagely consumes one bit. Thus, we use a fixed probability model for the coding of sign bits.

*5) End-of-Significant-Bit-Plane (EOSP):* The EOSP symbol notifies the end of significant bit coding in a bit-plane. The location of EOSP reveals the energy distribution in a transform block. Through the spatial correlation, we can predict the location of EOSP by taking the average of the zigzag indices from the EOSP symbols in the nearest four neighbors. Particularly, when the adjacent EOSP used for prediction is not reached yet, we use the zigzag index of the last nonzero significant bit as replacement. With the predicted location, we define the context model of EOSP symbol as the offset (range: $-7 \sim 7$) between the predicted EOSP location and the currently coded nonzero signifi-

TABLE II
CONTEXT MODEL OF THE SIGNIFICANT BIT

| Reference Factor | Definition | Range |
|---|---|---|
| Run | Distance between the previously coded nonzero significant bit and the current coding bit in zigzag order. | 0~7 |
| Sum of Significance Status | Summation of the co-located significance status in the nearest 4 blocks. | 0~4 |
| Frequency Band | Zigzag index of the current coding bit. | 0~10 |

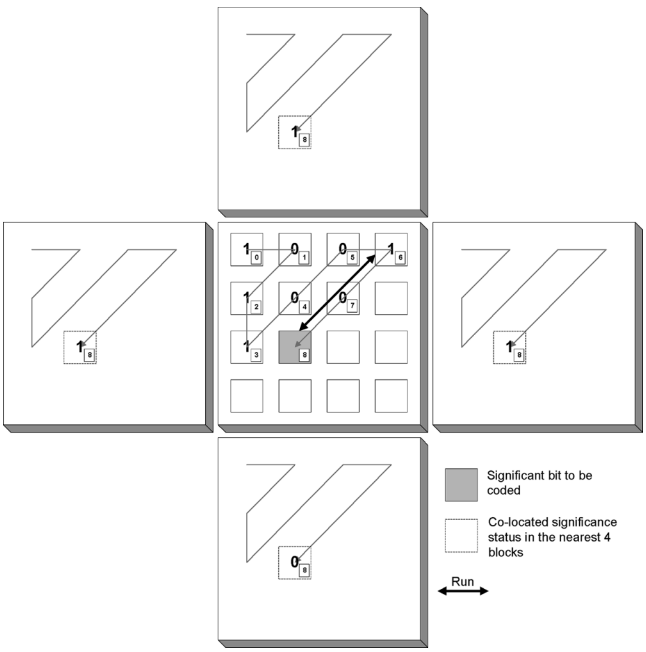


Fig. 2. Example of the context model for the significant bit. The transform block is with 4 × 4 integer transform.

cant bit. In addition, we jointly consider the bit-plane index as another factor since the distribution of offset values varies for each bit-plane. From the MSB bit-plane to the LSB bit-plane of a block, the bit-plane index is increased by one from zero. To save memory, the bit-plane index greater than 4 is truncated.

*6) Part_II_ALL_Zero:* The "Part_II_All_Zero" symbol notifies the decoder about the all zero case of Part II. Table I shows that such event is unevenly distributed. Moreover, the probability distribution varies for each bit-plane. Thus, we take the bit-plane index as the context model of Part_II_ALL_Zero symbol.

### *D. Context Dilution Problem*

In our CABIC, the number of context probability models increases with the transform size. For example, the context model of significant bit takes the coefficient zigzag index as one of the reference factors. Larger transform size requires more context probability models that cause context dilution problem. Experimental results show that the context dilution problem leads to worse coding efficiency. To reduce the number of context probability models, our CABIC adopts the 4 × 4 integer transform [14] for the coding of the enhancement layer.

### *E. Coding Flow Using Raster and Zigzag Scanning*

With the context model for each type of bits, the enhancement-layer frame is coded from the MSB bit-plane to the LSB bit-plane. In each bit-plane, the coding is performed in a frame raster and coefficient zigzag scanning manner. Specifically, the transform blocks in a frame are ordered with raster scanning and the coefficients in a block are coded in zigzag order.

Before the coding of each block, a MSB_REACHED symbol is first coded to notify if the MSB bit-plane of a block is reached. During the coding, different bit types are coded differently. If the input bit is a significant bit, we examine the partition to which the significant bit belongs. For a significant bit in Part I, we first code the significant bit by itself. When the coded significant bit becomes nonzero, we further code a sign bit. For a significant bit in Part II, we additionally code an EOSP bit after the sign bit. Particularly, a Part_II_ALL_Zero symbol is coded prior to the coding of the significant bits in Part II. When the Part_II_ALL_ZERO or the EOSP is true, the coding will be resumed from the next block. In addition, if the input bit is a refinement bit, we simply code the refinement bit by itself.

Experimental results show that our CABIC scheme offers a PSNR gain of 0.5$\sim$1.0 dB over the VLC-based bit-plane coding in MPEG-4 FGS [7]. However, although the objective quality (PSNR) is significantly improved, the poor subjective quality from the frame raster scanning still remains.

## III. STOCHASTIC BIT RESHUFFLING

To improve the subjective quality, we propose a content-aware SBR scheme. Instead of using the frame raster and coefficient zigzag scanning, we propose to reshuffle the coefficient bits of each bit-plane in a stochastic rate-distortion sense.

The concept and criterion of bit reshuffling was first proposed in [6] for improving the rate-distortion performance of wavelet-based image codec. For the reshuffling, in [6] each coefficient bit is first assigned with two factors that are the squared error reduction $\Delta D$ and the coding cost $\Delta R$. With these parameters, the coefficient bits are reshuffled such that the associated $(\Delta D/\Delta R)$ is in descending order. By the equal slope concept of rate-distortion optimization theory, such order leads to minimum distortion at any bit rates. However, the actual $\Delta D$ and $\Delta R$ of each coefficient bit are generally not available at decoder. Thus, the estimated $\Delta D$ and $\Delta R$ are used to avoid the transmission of coding order. With the same estimation scheme at both encoder and decoder, the coding order is implicitly known to both sides. Equation (1) shows the condition of optimal coding order in the stochastic rate-distortion sense, where $\widetilde{E}[\cdot]$ denotes taking estimation, the subscripts of $\Delta D$ and $\Delta R$ represents the bit identification, and the one of $(\widetilde{E}[\Delta D]/\widetilde{E}[\Delta R])$ specifies the coding order

$$\begin{aligned}\left(\frac{\widetilde{E}[\Delta D_i]}{\widetilde{E}[\Delta R_i]}\right)_1 &\geq \left(\frac{\widetilde{E}[\Delta D_j]}{\widetilde{E}[\Delta R_j]}\right)_2 \\ &\geq \left(\frac{\widetilde{E}[\Delta D_k]}{\widetilde{E}[\Delta R_k]}\right)_3 \geq \cdots\cdots\cdots \geq \left(\frac{\widetilde{E}[\Delta D_l]}{\widetilde{E}[\Delta R_l]}\right)_N. \qquad (1)\end{aligned}$$

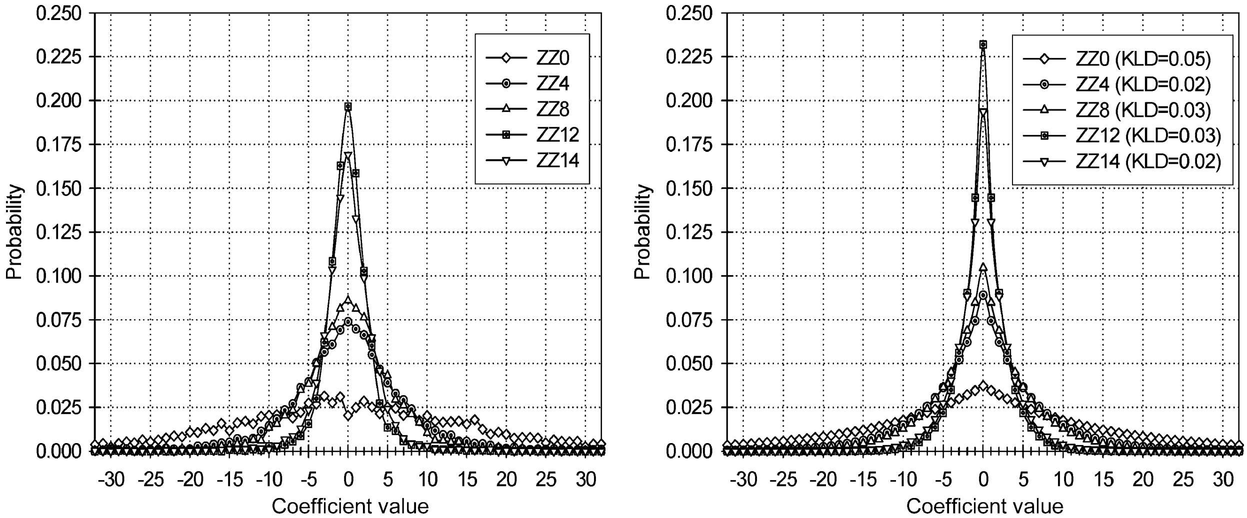


(a) (b)

Fig. 3. Probability distributions of the 4 × 4 integer transform coefficients. The legend ZZn denotes the zigzag index of a coefficient and the KLD stands for the Kullback–Leibler distance [2]. (a) Actual probability distributions. (b) Estimated probability models.

In this paper, we employ the same concept for the bit reshuffling at the enhancement layer. Particularly, our estimation incorporates the context probability model to make the priority assignment content aware so that the subjective quality can be improved. Moreover, we follow the optimized coding order in (1) to provide similar or even better rate-distortion performance.

## IV. Parameter Estimation

To estimate the $\Delta D$ and $\Delta R$ for a coefficient bit, we resort to their expected values. In this section, we show how we use a discrete Laplacian distribution and context probability models to estimate the rate-distortion function for a 4 × 4 integer transform coefficient.

### A. Discrete Laplacian Distribution

For calculating the expectations of $\Delta D$ and $\Delta R$, we need the probability distribution of each transform coefficient. Since the actual distribution is only available at encoder side, we adopt a model-based approach to minimize the overhead. Specifically, we model each 4 × 4 integer transform coefficient with a discrete Laplacian distribution, as defined in (2), where $X_{n,k}$ denotes the $n$th zigzag-ordered coefficient of block $k$ and $x_{n,k}$ stands for its outcome. Particularly, we assume the co-located coefficients are independently and identically distributed (i.i.d.). Thus, the Laplacian parameter $\alpha_n$ only depends on the zigzag index $n$

$$P[X_{n,k} = x_{n,k}] \triangleq \frac{1-\alpha_n}{1+\alpha_n} \times (\alpha_n)^{|x_{n,k}|}. \tag{2}$$

To estimate the Laplacian parameter, we use maximum likelihood principle. Given a set of $M$ observed data and a presumed joint probability with an unknown parameter, the maximum likelihood estimator for the unknown parameter is the one that maximizes the joint probability. For an enhancement-layer frame with $M$ 4 × 4 blocks, the joint probability for the $n$th zigzag-ordered coefficients can be written as in (3). According to the i.i.d. assumption, we can simplify the joint probability as $M$ multiplication terms. Further, by substituting (2) into (3), we can obtain a close form formula for the joint probability as follows:

$$\begin{aligned} &P[X_{n,1} = x_{n,1}, X_{n,2} = x_{n,2}, \ldots, X_{n,M} = x_{n,M}] \\ &\quad = P[X_{n,1} = x_{n,1}] \times P[X_{n,2} = x_{n,2}] \ldots \\ &\quad\quad \times P[X_{n,M} = x_{n,M}] \\ &\quad = \left(\frac{1-\alpha_n}{1+\alpha_n}\right)^M \times (\alpha_n)^{\sum_{k=1}^{M} |x_{n,k}|}. \end{aligned} \tag{3}$$

By definition, the maximum likelihood estimator of $\alpha_n$ is the one that maximizes (3). To find the solution, we take the derivative with respect to $\alpha_n$ and solve for the root. We leave the detail derivation in Appendix A. Based on (3), (4) shows our maximum likelihood estimator for the $\alpha_n$

$$\alpha_n = -\mu_X^{-1} + \sqrt{\left(\mu_X^{-1}\right)^2 + 1}, \text{ where } \mu_X = \frac{\sum_{k=1}^{M} |x_{n,k}|}{M}. \tag{4}$$

According to (4), to estimate the $\alpha_n$ for a coefficient, we first calculate the mean of absolute values of the co-located coefficients, $\mu_X$, and then substitute it into (4) to obtain the estimator. Specifically, the estimation is done at the encoder and the estimated parameters are transmitted to the decoder. For each enhancement-layer frame, we have 16 parameters for the luminance component and another 16 parameters for the chrominance part. Particularly, each parameter is quantized and coded with a 8-bit syntax at frame level. Thus, for each enhancement-layer frame, additional 256 bits are coded as overhead. As compared to the entire bit-stream, the overhead is just a minor portion.

Fig. 3 compares the estimated distributions with the actual ones. As shown, the actual distributions are close to Laplacian and the estimated models preserve the relative distributions of different coefficients. To show the accuracy of our estimation,

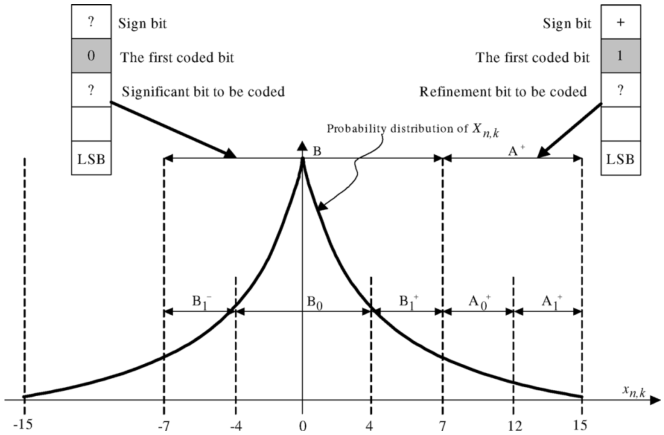


Fig. 4. Examples of $\Delta D$ estimation for the significant bit and refinement bit.

we calculate the Kullback–Leibler distance[1] (KLD) [2], which is a common measure for showing the difference between the actual distribution and its estimation. A KLD of value 0 means that the estimated distribution is identical to the actual one. As shown in Fig. 3(b), the KLD between our estimated distributions and the actual ones approaches zero; that is, our estimated distributions are close to the actual ones.

### B. Estimation of Delta Distortion

To estimate the $\Delta D$ for a coefficient bit, we use the reduction of expected squared error. Since the decoding of a coefficient bit is to reduce the uncertainty for a coefficient, we can calculate the reduction of expected squared error from the decrease of uncertainty interval.

Fig. 4, we depict the estimated distribution of a 4-bit coefficient and give two examples for illustrating the decrease of uncertainty interval. Without loss of generality, the left-hand side shows an example of a significant bit, where the first bit is coded as zero. On the other hand, the right-hand side illustrates the case of refinement bit, where the first bit is nonzero.

From the coded bits, we can identify the uncertainty interval in which the actual value is located. For instance, in the example of significant bit, we know that the actual value is confined within the interval $B$. Similarly, for the case of refinement bit, we learn that the actual value falls in the interval $A^+$. Given the interval derived from the previously coded bits, the next bit for coding is to further decrease the uncertainty interval. For example, the significant bit to be coded is to determine that the actual value is in the subinterval $B_0$ or $\{B_1^+ \cup B_1^-\}$. Particularly, for a significant bit of nonzero, an additional sign bit is coded to further decide that the actual value is in the subinterval $B_1^+$ or $B_1^-$. By the same token, the refinement bit to be coded is to determine that the actual value is in the subinterval $A_1^+$ or $A_0^+$.

From the decrease of uncertainty interval, we can calculate the reduction of expected squared error. At decoder side, the expected squared error in an interval is the variance within the interval. Thus, we can express our $\Delta D$ estimation as the reduction of variance. Equation (5) formulates our $\Delta D$ estimation for the case of significant bit in Fig. 4, where $\mathrm{Var}[X_{n,k}|X_{n,k} \in B]$ denotes the conditional variance of $X_{n,k}$ given that $X_{n,k}$ is in the interval $B$. Similarly, we have the variances for the subintervals $B_1^+$, $B_1^-$, and $B_0$. Since we do not know in which subinterval the actual value is located, the variance of each subinterval is further weighted by its probability. To simplify the expression, we find that the variances of $B_1^+$ and $B_1^-$ are identical because Laplacian distribution is symmetric. So, we can merge the second and the third terms in (5) by factorization. Appendix B gives the detail derivations for the conditional probability and conditional variance in terms of interval range and $\alpha_n$

$$
\begin{aligned}
&\widetilde{E}[\Delta D_{n,k,B,\mathrm{significant}}] \\
&\quad \triangleq \mathrm{Var}[X_{n,k}|X_{n,k} \in B] \\
&\qquad - P\left[X_{n,k} \in B_1^+|X_{n,k} \in B\right] \times \mathrm{Var}\left[X_{n,k}|X_{n,k} \in B_1^+\right] \\
&\qquad - P\left[X_{n,k} \in B_1^-|X_{n,k} \in B\right] \times \mathrm{Var}\left[X_{n,k}|X_{n,k} \in B_1^-\right] \\
&\qquad - P\left[X_{n,k} \in B_0|X_{n,k} \in B\right] \times \mathrm{Var}[X_{n,k}|X_{n,k} \in B_0] \\
&\quad = \mathrm{Var}[X_{n,k}|X_{n,k} \in B] \\
&\qquad - \big(P\left[X_{n,k} \in B_1^+|X_{n,k} \in B\right] \\
&\qquad\qquad + P\left[X_{n,k} \in B_1^-|X_{n,k} \in B\right]\big) \\
&\qquad \times \mathrm{Var}\left[X_{n,k}|X_{n,k} \in B_1^+\right] \\
&\qquad - P[X_{n,k} \in B_0|X_{n,k} \in B] \times \mathrm{Var}[X_{n,k}|X_{n,k} \in B_0]. \qquad (5)
\end{aligned}
$$

In (5), the co-located significant bits within the same interval have the same estimated $\Delta D$ because the co-located coefficients have identical Laplacian model. The priorities of the co-located significant bits may not be distinguishable. To perform the reshuffling in a content-aware manner so that the regions containing more energy are with higher priority, in (5) the subinterval probabilities are replaced with the context probability models. Recall that the context model of significant bit refers to the significance status of the adjacent and co-located coefficients. Using the context probability model for substitution makes the $\Delta D$ estimation become content aware and energy dependent.

For the substitution of subinterval probabilities in (5), we find that $(P[X_{n,k} \in B_1^+|X_{n,k} \in B] + P[X_{n,k} \in B_0|X_{n,k} \in B])$ actually denotes the probability of nonzero for the significant bit to be coded and $P[X_{n,k} \in B_0|X_{n,k} \in B]$ represents its probability of zero. Hence, we use the associated context probability models to substitute for these two terms. Equation (6) shows the content-aware $\Delta D$ estimation for the example of significant bit in Fig. 4, where $SigCtxP(CtxIdx(n,k,B),1)$ denotes the context probability of nonzero for the significant bit of $X_{n,k}$ that locates in the interval $B$. Correspondingly, the $SigCtxP(CtxIdx(n,k,B),0)$ represents its probability of zero.

$$
\begin{aligned}
&\widetilde{E}[\Delta D_{n,k,B,\mathrm{significant}}] \\
&\quad \cong \mathrm{Var}[X_{n,k}|X_{n,k} \in B] \\
&\qquad - SigCtxP\left(CtxIdx(n,k,B),1\right) \\
&\qquad \times \mathrm{Var}\left[X_{n,k}|X_{n,k} \in B_1^+\right] \\
&\qquad - SigCtxP\left(CtxIdx(n,k,B),0\right) \\
&\qquad \times \mathrm{Var}[X_{n,k}|X_{n,k} \in B_0]. \qquad (6)
\end{aligned}
$$

[1] $KLD(P(x),\widetilde{P}(x)) = \sum_x P(x)\log_2(P(x)/\widetilde{P}(x))$, where $P(x)$ is the actual probability distribution and $\widetilde{P}(x)$ is its estimation.

Following the same procedure, one can estimate the $\Delta D$ for the other bits. Equation (7) shows the estimated $\Delta D$ for the case of refinement bit in Fig. 4. Since the refinement bit does not have any context probability model, the conditional probabilities in (7) are derived from an estimated Laplacian model

$$\begin{aligned}
&\widetilde{E}[\Delta D_{n,k,A^+,\text{refinement}}] \\
&\quad \triangleq \text{Var}[X_{n,k}|X_{n,k}\in A^+] \\
&\qquad - P\left[X_{n,k}\in A_1^+|X_{n,k}\in A^+\right] \\
&\qquad \times \text{Var}\left[X_{n,k}|X_{n,k}\in A_1^+\right] \\
&\qquad - P\left[X_{n,k}\in A_0^+|X_{n,k}\in A^+\right] \\
&\qquad \times \text{Var}\left[X_{n,k}|X_{n,k}\in A_0^+\right]. \qquad (7)
\end{aligned}$$

### C. Estimation of Delta Rate

To estimate the $\Delta R$ for a coefficient bit, we use the binary entropy[2], which represents the minimum expected coding bit rate for an input bit. Equation (8) defines our $\Delta R$ estimation for the significant bit in Fig. 4. The first term represents the binary entropy of a significant bit using the context probability model as an argument while the second term denotes the cost from a sign bit. The sign bit is considered as partial cost of the significant bit because the decoder can only perform the reconstruction after the sign is received. Recall that each sign bit averagely consumes one bit. Also, the sign bit is only coded after a significant bit of nonzero. Thus, the cost of the sign bit is weighted by the context probability model of nonzero

$$\begin{aligned}
\widetilde{E}[\Delta R_{n,k,B,\text{significant}}] \triangleq\, & H_b(SigCtxP(CtxIdx(n,k,B),1)) \\
& + SigCtxP\left(CtxIdx(n,k,B),1\right)\times 1. \qquad (8)
\end{aligned}$$

In addition, (9) illustrates our $\Delta R$ estimation for the example of refinement bit. To calculate the binary entropy, we use the conditional probability of a subinterval as an argument. For instance, we use $P[X_{n,k}\in A_1^+|X_{n,k}\in A^+]$ as an argument in (9). In particular, as mentioned in Section II, such an estimated probability is not only for the calculation of binary entropy, but also for the CABIC coding. By the same methodology, one can estimate the $\Delta R$ for the other bits

$$\widetilde{E}[\Delta R_{n,k,A^+,\text{refinement}}] \triangleq H_b\left(P\left[X_{n,k}\in A_1^+|X_{n,k}\in A^+\right]\right). \qquad (9)$$

## V. Dynamic Priority Management for Stochastic Bit Reshuffling

Given the estimated rate-distortion performance for each coefficient bit, in this section, we further show how these data are used for the SBR. Firstly, we illustrate our constraints for the reshuffling. Then, we present the dynamic priority management for the SBR. Lastly, we use an example to illustrate the idea.

### A. Constraints of Reshuffling Order

In our algorithm, we pose two constraints on the reshuffling order to maintain low complexity and high coding efficiency. These constraints make our implementation suboptimal in the stochastic rate-distortion sense. Specifically, they are as follows.

- *For an enhancement-layer frame, the coding is conducted sequentially from the MSB bit-plane to the LSB bit-plane.* This constraint is to keep low complexity. Ideally, the reshuffling should allow the coefficient bits at different bit-planes be coded in an interleaved manner. However, in practical implementation, such flexibility requires a huge amount of coding states and branch instructions. Thus, in this paper, we perform the SBR in a bit-plane by bit-plane manner.
- *For each bit-plane of a transform block, the coding of the significant bits in Part II always follows zigzag order.* This constraint is to maintain high coding efficiency. Recall that the coding of the significant bits in Part II will stop as the actual EOSP is reached. Since the location of EOSP is not known in advance, we follow zigzag order for the coding of the significant bits in Part II to prevent the redundant bits after EOSP from coding.

### B. Dynamic Priority Management

To maintain the coding priority, we implement two dynamic coding lists for the reshuffling of significant bits and refinement bits. Each type of bits in the associated list allocates a register to record its bit location and estimate rate-distortion data. For synchronization, both encoder and decoder follow the same procedure to manage the lists. Sequentially, the management scheme includes the following five steps.

1) **Coding List Initialization**: Before the coding of each bit-plane, we estimate the rate-distortion data for the following bits and put them in the associated coding lists: 1) all the significant bits in Part I; 2) all the first zigzag-ordered significant bits in Part II; and 3) all the refinement bits in the current bit-plane.
2) **Coding List Reshuffling**: After the initialization, we perform the reshuffling, according to the estimated rate-distortion data, to identify the highest priority bit in the lists, i.e., the one with maximum $(\widetilde{E}[\Delta D]/\widetilde{E}[\Delta R])$. In addition, the reshuffling is performed after the coding of each bit.
3) **Binary Arithmetic Coding**: Once the highest priority bit is identified, we follow the CABIC scheme in Section II for coding.
4) **Rate-Distortion Data Update**: After the coding of a nonzero significant bit, we update parts of the rate-distortion data in the list of significant bit. Such update is to guarantee that our priority assignment is based on the latest context probability model. Moreover, through the update, we can fully utilize the coded information to enhance the effectiveness of content-aware bit reshuffling. Specifically, whenever a significant bit of nonzero is coded, we search in the coding list and update the registers for the following significant bits.
   - Category 1: The significant bits that have the same context index as the current coded one.
   - Category 2: The co-located significant bits in the adjacent blocks.
   - Category 3: The significant bits in Part I that locate after the current coded one (in zigzag order).

[2] $H_b(P(1)) = -P(1)\times\log_2(P(1)) - (1-P(1))\times\log_2(1-P(1))$, where P(1) is the nonzero probability of the coding bit.

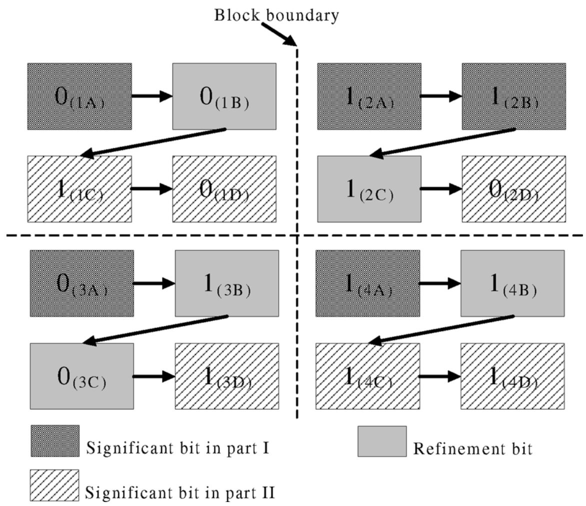


Fig. 5. Example of dynamic bit reshuffling in a bit-plane.

TABLE III
LIST OF THE SIGNIFICANT BIT DURING THE BIT RESHUFFLING

| Content of Significant Bit List | | | The Reshuffling Result | | |
|---|---|---|---|---|---|
| Bit | Context | Priority | Bit | Context | Priority |
| After Initialization | | | | | |
| 1A | (0, 0) | 3 | 1C | (2, 0) | 5 |
| 1C | (2, 0) | 5 | 4C | (2, 0) | 5 |
| 2A | (0, 0) | 3 | 2B | (2, 1) | 4 |
| 2B | (2, 1) | 4 | 1A | (0, 0) | 3 |
| 2D | (0, 0) | 3 | 2A | (0, 0) | 3 |
| 3A | (0, 0) | 3 | 2D | (0, 0) | 3 |
| 3D | (0, 0) | 3 | 3A | (0, 0) | 3 |
| 4A | (0, 0) | 3 | 3D | (0, 0) | 3 |
| 4C | (2, 0) | 5 | 4A | (0, 0) | 3 |
| After (1C, 4C) are coded, 4D is included | | | | | |
| 2B | (2, 1) | 4 | 2B | (2, 1) | 4 |
| 1A | (0, 0) | 3 | 1A | (0, 0) | 3 |
| 2A | (0, 0) | 3 | 2A | (0, 0) | 3 |
| 2D | (0, 0) | 3 | 2D | (0, 0) | 3 |
| 3A | (0, 0) | 3 | 3A | (0, 0) | 3 |
| 3D | (0, 0) | 3 | 3D | (0, 0) | 3 |
| 4A | (0, 0) | 3 | 4A | (0, 0) | 3 |
| **4D** | **(0, 0)** | **3** | **4D** | **(0, 0)** | **3** |
| After (2B, 1A, 2A) are coded, 4A is updated | | | | | |
| 2D | (0, 0) | 3 | **4A** | **(1, 0)** | **4** |
| 3A | (0, 0) | 3 | 2D | (0, 0) | 3 |
| 3D | (0, 0) | 3 | 3A | (0, 0) | 3 |
| **4A** | **(1, 0)** | **4** | 3D | (0, 0) | 3 |
| 4D | (0, 0) | 3 | 4D | (0, 0) | 3 |
| After 4A is coded, 3A is updated | | | | | |
| 2D | (0, 0) | 3 | **3A** | **(1, 0)** | **4** |
| **3A** | **(1, 0)** | **4** | 2D | (0, 0) | 3 |
| 3D | (0, 0) | 3 | 3D | (0, 0) | 3 |
| 4D | (0, 0) | 3 | 4D | (0, 0) | 3 |

Updating the significant bits of Category 1 is necessary since the context probability model is refined after the coding. By the same token, updating the significant bits of Categories 2 and 3 is essential because the associated context indices have changed. Recall that the context model of significant bit refers to the significance status of the adjacent and co-located coefficients. Since all the coefficients are initialized with insignificant status, the context indices for those significant bits in Categories 2 and 3 are changed as the coded coefficient becomes significant. Therefore, we must update their rate-distortion data. Particularly, the rate-distortion data of the refinement bit is not required for update because it is derived from the estimated Laplacian model, which is fixed throughout the reshuffling process.

5) **Significant Bit Inclusion**: From our reshuffling constraints, the coding of the significant bits in Part II always follows zigzag order. Thus, whenever a significant bit in Part II is coded, we estimate the rate-distortion data for the next zigzag-ordered significant bit and put it in the list.

To complete the coding of a bit-plane, Steps 2$\sim$5 are repeated. When the coding of a bit-plane is done, we repeat Steps 1$\sim$5 until all the bit-planes are coded.

For better understanding, in Fig. 5, we use an example to illustrate the reshuffling process, where the binary number in each rectangle represents the content of a coefficient bit and its subscript denotes the bit identification. For simplicity, we only illustrate the reshuffling of significant bits. One can follow the same procedure to reshuffle the refinement bits. Practically, after the reshuffling of each list, we compare the highest priority bit in each list to identify the one for coding.

In the example of Fig. 5, we simplify the priority calculation as the summation of "(3-Run)" and the "Sum of Significance Status" that is defined in Table II. With our definition, the coefficient bits that have a shorter run and more significant coefficients in the adjacent blocks will be assigned with higher coding priority. Specifically, to calculate the priority for each bit, the significant bits to be coded are first initialized with insignificant status and the refinement bits are considered as significant. Thus, for the bit 1C, its "Sum of Significance Status" is 2 and its "Run" index is 0. According to our definition, the bit 1C has a priority value of 5. By the same procedure, the priorities for the other significant bits can be obtained.

In Table III[3], we present the content of significant bit list for the example in Fig. 5. On the right-hand side of Table III, we show the reshuffling result based on the coding priority. As shown, for the initialization, the coding list first includes the significant bits in Part I and the first zigzag-ordered significant bits in Part II. Then, according to the priority, the reshuffling is performed. Table III shows that 1C has the highest priority after the reshuffling. Hence, we start the coding form the 1C. After 1C is coded, we skip Step 4 because the adjacent and co-located coefficients have become significant. There are no significant bits to be updated. In addition, Step 5 is also skipped since 1C is the EOSP of a block. As a result, after the coding of 1C, we directly perform the coding for 4C. Particularly, after 4C is coded, we skip Step 4 for the same reason as the 1C. However, we include 4D in the list according to Step 5. The following 2B, 1A, and 2A are coded similarly. But, after 2A is coded and becomes nonzero, we update the rate-distortion data of 4A according to Step 4. As illustrated in Table III, the 4A becomes the one with the highest priority after the update and reshuffling. Therefore, we resume the coding from 4A. By continuing the procedure, one can finish the coding of significant bits and obtain the coding order as $(1C \rightarrow 4C \rightarrow 2B \rightarrow 1A \rightarrow 2A \rightarrow 4A \rightarrow 3A \rightarrow 2D \rightarrow 3D \rightarrow 4D)$. In particular, with the reshuffling, 2B is coded prior to 2A, which means that the significant bits in Part I could be coded in an order other than zigzag. We

[3]Context=(Summation of co-located significance status in the nearest four blocks Run).

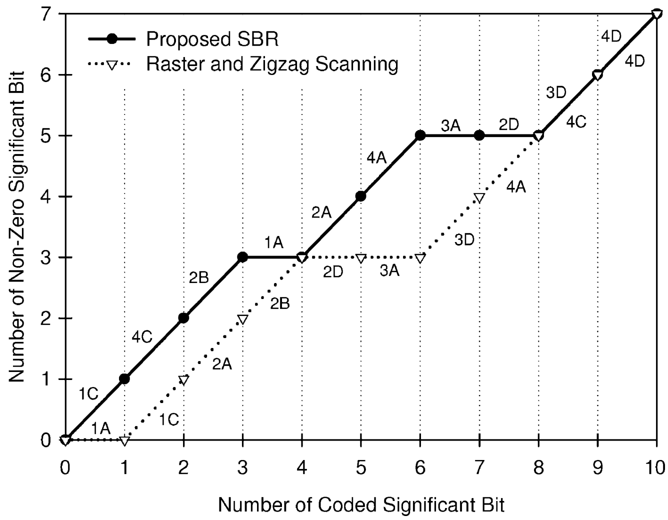


Fig. 6. Comparison of number of nonzero significant bits with different coding orders.

use such flexibility to allow optimization. As compared to the frame raster and coefficient zigzag scanning, (1A $\rightarrow$ 1C $\rightarrow$ 2A $\rightarrow$ 2B $\rightarrow$ 2D $\rightarrow$ 3A $\rightarrow$ 3D $\rightarrow$ 4A$\rightarrow$ 4C $\rightarrow$ 4D), Fig. 6 shows that our SBR has more significant bits of nonzero among the same number of coded significant bits. Generally, a significant bit of nonzero contributes more to the error reduction at decoder.

## VI. Dynamic Memory Organization

The reshuffling and update process causes intensive computation. With straightforward implementation, the estimated rate-distortion data of all coefficient bits must be updated after the coding of a nonzero significant bit; then, the reshuffling is conducted using all coefficient bits as input. From the profiling of foreman CIF sequence on P4 2.0-GHz machine, it takes about 30 min for the bit-plane encoding[4] of an enhancement-layer frame, which is unacceptable and unrealistic. Thus, in this section, we propose a dynamic memory organization to reduce the complexity of SBR.

### *A. Memory Management for the List of Significant Bit*

For reducing the complexity of update and reshuffling, we observe that not all the registers are required for modification after the coding of a nonzero significant bit. Thus, we can minimize the computation by updating those outdated registers while keeping the others untouched.

To update the outdated registers, we first search them in the list. To quickly identify the registers of Category 1, we group the registers recording the same context index by a linked list. The right-hand side of Fig. 7 shows an example, where each circle denotes the associated register of a significant bit and each rectangle represents a context group. In each group, the registers with the same context index are grouped by a linked list. In addition, to identify the registers of Categories 2 and 3, we avoid exhaustive searching by confining our search within certain context groups. To determine which context groups for search, we follow the definitions of Categories 2 and 3 to derive the bit locations for those outdated significant bits. From the bit locations, we further calculate their context indices before the coding by reversing the significance status of the currently coded bit. These context indices then determine the context groups for search. Within a group, we perform the search by comparing the bit location. Then, we update the outdated rate-distortion data using the latest context probability model.

[4]The bit-plane coding at the enhancement layer has balanced complexity in encoder and decoder.

After the update, we perform the reshuffling in a hierarchical way. Specifically, we first identify the highest priority bit in each group. Then, we assign each group a context group pointer that points to the highest priority bit in a group. Lastly, we reshuffle the context group pointers to find out the highest priority bit in the list. Note that we do not directly reshuffle the highest priority bit of each group since we want to maintain the same context group structure. Particularly, the reshuffling in each group and the reordering of all the context group pointers are performed in the initialization step. During the actual coding, we only modify certain context groups and context group pointers so that the computation for reshuffling is minimized. Fig. 7 shows an example of our priority structure. For each group, the priority from left to right is in descending order. Similarly, for different groups, the priority of the highest priority bit from top to bottom is in descending order, i.e., we have $\mathrm{A3} > \mathrm{A1} > \mathrm{A5} > \ldots . > \mathrm{AN}$. In this example, A3 is not only the highest priority bit of Ctx3 group, but also has the highest priority in the list.

During the reshuffling and update, we must quickly access a context group for a given context index. To avoid exhaustive search in the linked list of context group pointers, we construct a look-up table that takes the context index as input and produces the associated context group pointer. The left-hand side of Fig. 7 depicts an example of the look-up table.

To show our dynamic memory organization, we use Fig. 7 as an example, where we assume that the registers in each group and the context group pointers have been reshuffled since the initialization. According to our priority structure, we start the coding from A3. Moreover, we assume the context indices of relevant registers B5 and A2 must be changed as A3 is recognized significant. To perform the reshuffling, after A3 is coded, we first update the rate-distortion data for the registers in the same group, i.e., B3, C3, and D3. Next, we update the rate-distortion data of B5 and A2. Then we move B5 and A2 to the other context groups since their context indices have been changed. Specifically, the destination groups are determined by their context indices after A3 becomes significant. For example, in Fig. 7, the register B5 is updated and moved from the Ctx5 group to the B4 position of the Ctx4 group. Similarly, the register A2 is updated and moved from the Ctx2 group to the Ctx6 group. Particularly, we put B5 at the location of B4 because the priority in the Ctx4 group is $\mathrm{A4} > \mathrm{B5}\ (\mathrm{B4}) > \mathrm{C4}$.

After the update and movement for the relevant context groups (i.e., Ctx groups 3, 5, 2, 4, and 6), the highest priority bits of Ctx3, Ctx2, and Ctx6 groups have been changed. Thus, we must determine their new positions in the linked list of the context group pointers. To do so, we first remove the context group pointers (i.e., Context group pointers 3, 2, and 6) from the linked list. Then, we sequentially insert them back at proper positions by comparing the registers of the highest priority

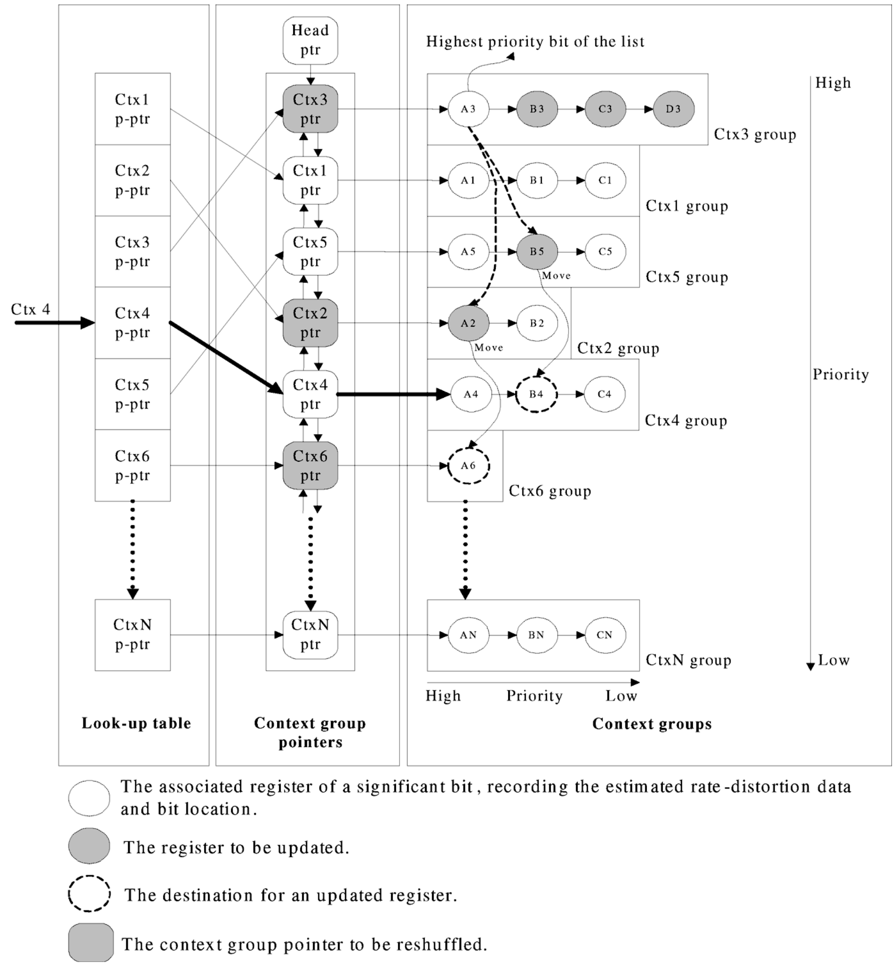


Fig. 7. Dynamic memory organization for the list of the significant bit.

TABLE IV
AVERAGE EXECUTION TIME FOR THE BIT-PLANE ENCODING OF AN ENHANCEMENT-LAYER FRAME ON P4 2.0-GHz MACHINE

| Sequences | Straightforward Implementation | Dynamic Memory Organization | Improvement Ratio |
|---|---|---|---|
| Foreman_CIF | 1817 seconds | 38 seconds | 48 |
| Mobile_CIF | 2324 seconds | 37 seconds | 63 |
| News_CIF | 1662 seconds | 34 seconds | 49 |

TABLE V
ENCODER PARAMETERS FOR THE EXPERIMENTS

| Sequence | Foreman | Mobile | News |
|---|---|---|---|
| Base-layer Qp | 38(QCIF)/46(CIF) | 38 | 45 |
| Enh.-layer Prediction Bit Rate, QCIF | 128kbits/s | 160kbits/s | 64kbits/s |
| Enh.-layer Prediction Bit Rate, CIF | 320kbits/s | 384kbits/s | 256kbits/s |
| Frame Size | CIF (352x288) / QIF (176x144) | | |
| Frame Rate | 10 frames/s | | |
| GOP Structure | IPPPP…..P | | |
| Prediction Leaky Factor | 0.9375 | | |
| Reference Frame Number | 1 | | |
| Motion Estimation Range | 32 | | |
| Block Modes | All the block modes are enabled | | |
| Base-layer Entropy Coding Mode | CABAC | | |
| Freq. Weighting Matrix in Zigzag Order | (3, 3, 3, 2, 2, 2, 2, 2, 2, 2, 1, 1, 1, 1, 1, 1, 1, 1, 1, 1, 1, 0,…,0) | | |

after the update. Particularly, the linked list of context group pointers is bidirectional. We can easily remove any context group pointer from the list. In this example, we only modify the contents of the context groups 3, 5, 2, 4, and 6 while keeping the others untouched. The computation for update and reshuffling is minimized.

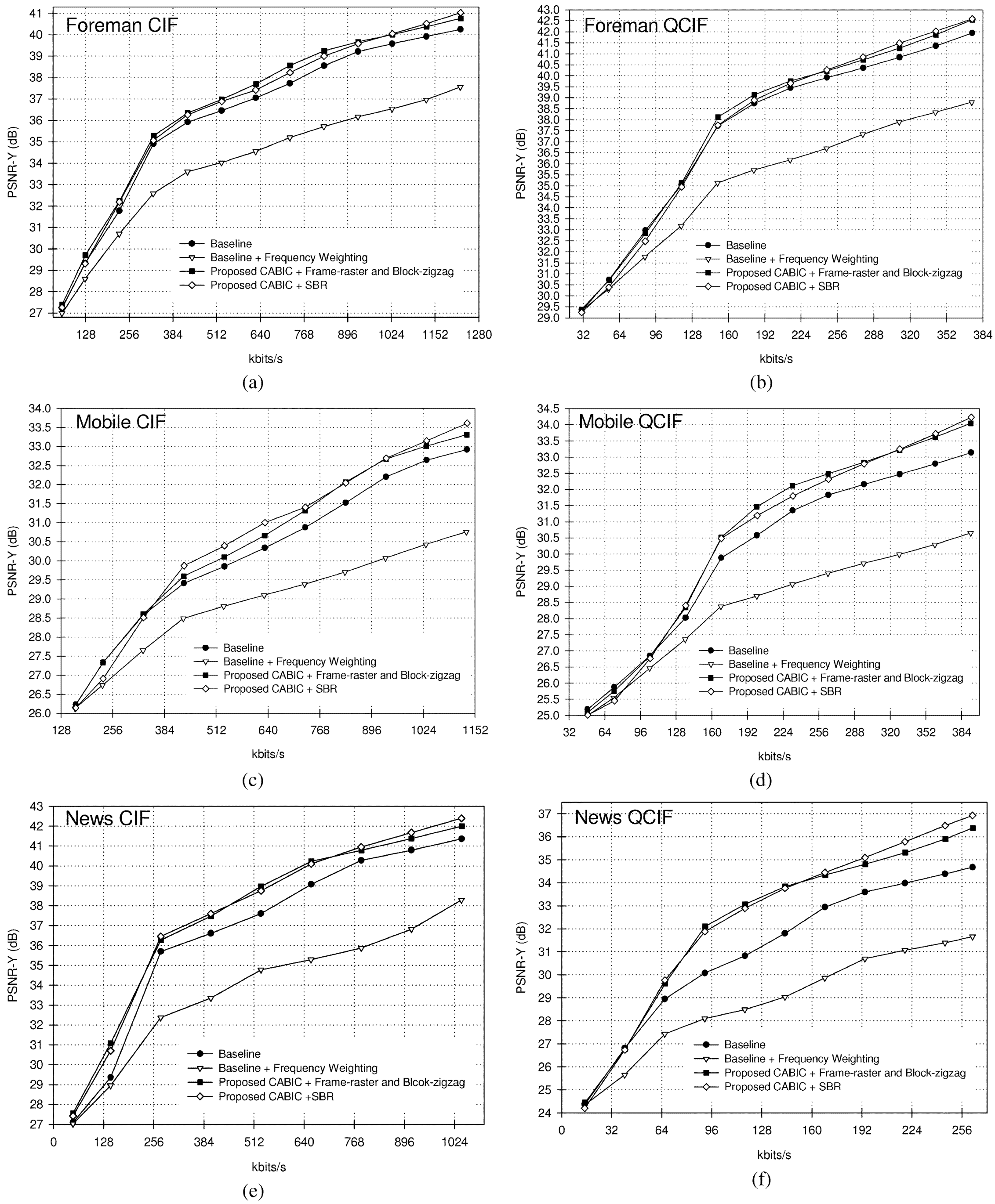


Fig. 8. Luminance PSNR comparison of baseline (VLC-based bit-plane coding in MPEG-4 FGS), baseline with frequency weighting, the proposed CABIC with frame raster and coefficient zigzag scanning, and the proposed CABIC with SBR.

### B. Memory Management for the List of Refinement Bit

For the refinement bit, we only reshuffle the registers for identifying the highest priority one. There is no need for update and relocation. Thus, we simply use a linked list to maintain the list of the refinement bit.

As compared to straightforward implementation, Table IV shows that a relative improvement ratio of more than 48× is achieved. Although the performance is still far way from real-time, more improvements are expected by further optimizing in both algorithmic and coding aspects.

## VII. Experiments

In this section, we assess the rate-distortion performance and subjective quality of our proposed scheme. For a fair comparison, all the schemes implemented adopt H.264 JM4 [14] as the base layer and RFGS [4] as the prediction scheme for the enhancement layer. Specifically, we use the VLC-based bit-plane coding [7] as baseline. Moreover, we show the performance of baseline with frequency weighting. To compare the rate-distortion performance, our decoder truncates the bit-stream of the enhancement layer at multiple bit rates and measures the PSNR of

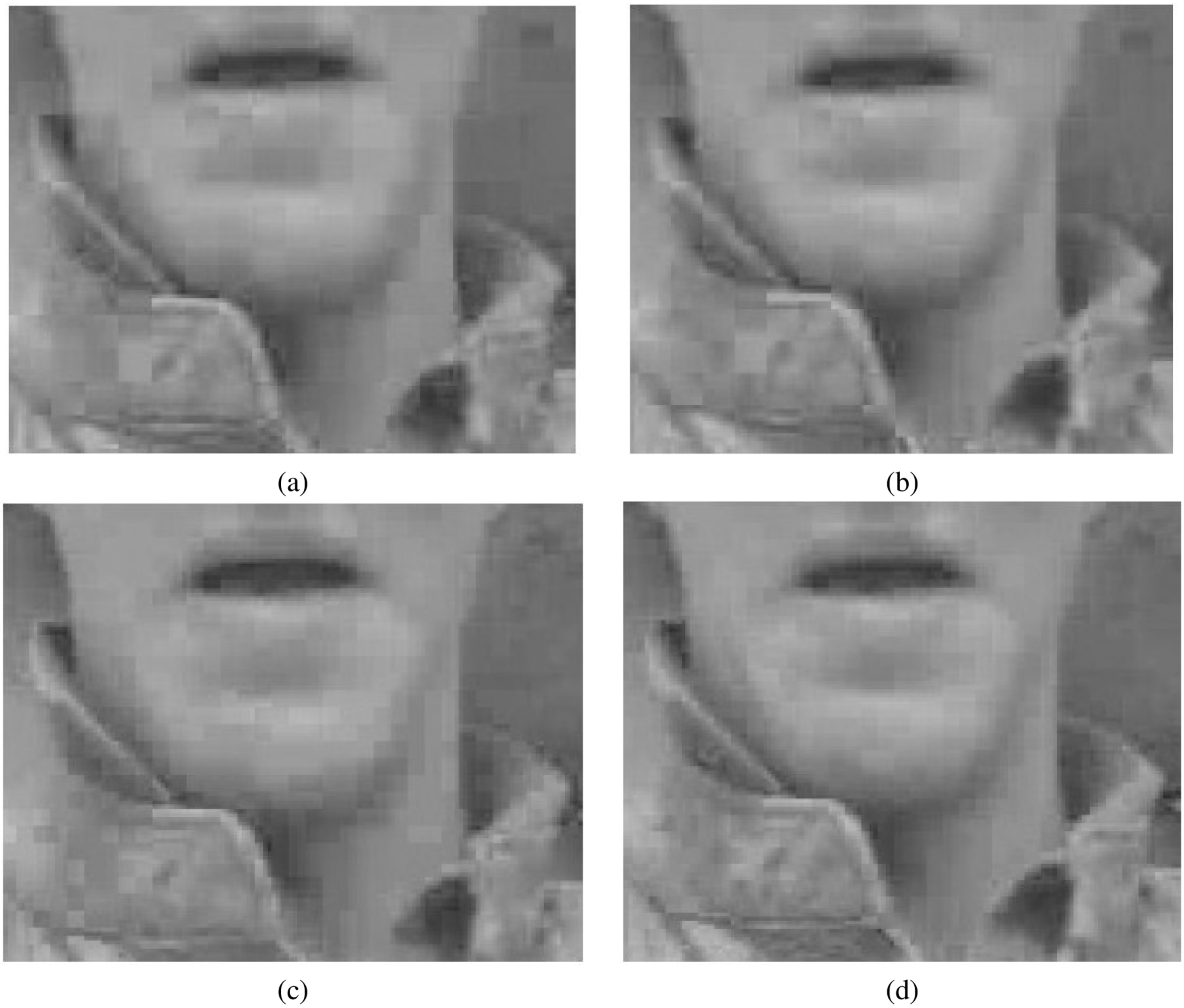

Fig. 9. Subjective quality comparison of the 94th frame in Foreman CIF sequence with bit rate at 255 kbits/s. (a) Baseline (VLC-based bit-plane coding in MPEG-4 FGS). (b) Baseline with frequency weighting. (c) Proposed CABIC with frame raster and coefficient zigzag scanning. (d) Proposed CABIC with SBR.

decoded video respectively. In addition, to compare the subjective quality, we show the decoded frames of different approaches at the same bit rate. Table V lists our encoder parameters. For each sequence, different coding schemes use identical encoder parameters. In particular, to setup the frequency weighting matrix for the baseline, we follow the rule in [7] to have the coefficients of a lower frequency be coded with higher priority.

In Fig. 8, we compare the PSNR of different approaches at various bit rates. As shown, enabling the frequency weighting on the baseline causes a PSNR loss of 2$\sim$3 dB. Conversely, as compared to the baseline, our CABIC with frame raster and coefficient zigzag scanning improves the PSNR by 0.5$\sim$1.0 dB at medium and high bit rates. Particularly, up to 2 dB gain can be observed in the News QCIF sequence. On the other hand, at the lower bit rates, the gain is less significant because the truncation of the enhancement layer causes drifting errors [4] and the proposed CABIC takes time for the convergence of context probability models. In addition, our SBR can further offer up to 0.2$\sim$0.5 dB improvement.

While maintaining similar or even higher coding efficiency, our SBR offers better subjective quality. Fig. 9 shows the comparison of visual quality using Foreman CIF sequence. For better assessment, we have enlarged the regions where the subjective quality shows noticeable differences. As shown, the baseline and our CABIC with frame raster and coefficient zigzag scanning reveal obvious blocking artifact. On the other hand, the frequency weighting can provide smoother quality. But, the edge and texture parts are blurred because the coefficients of higher frequency are always with lower coding priority. In contrast, our CABIC with content-aware SBR not only provides more uniform quality, but also keeps the details of edge and texture.

## VIII. Conclusions

In this paper, we propose a CABIC with a SBR scheme to deliver higher coding efficiency and better subjective quality for FGS video coding. For higher coding efficiency, we construct context models based on both the energy distribution in a block and the spatial correlations in the adjacent blocks. Moreover, we exploit the context across bit-planes to save side information. Experimental results show that our CABIC provides a PSNR gain of 0.5∼1.0 dB over the VLC-based bit-plane coding [7].

Further, for better subjective quality, our SBR combines context probability models and estimated Laplacian distributions to reorder coefficient bits in such a way that the estimated rate-distortion performance is in descending order. As compared to the approaches with frame raster and coefficient zigzag scanning, our SBR provides better visual quality and maintains similar or even higher coding efficiency.

This work proves that the bit-plane coding in MPEG-4 FGS [7] can be further improved in coding efficiency and subjective quality by additional complexity. However, as compared to the nonscalable H.264 [14], there is still a performance gap of 2∼4 dB with our testing conditions. To further reduce the gap, the proposed scheme can be improved with the stack FGS algorithms and hierarchical prediction schemes [3], [12] used in the current scalable video coding standard.

In addition to coding efficiency and subjective quality, another important issue that is not discussed in this paper is error resilience. Due to the data dependency from the context models and the nature of arithmetic coding, the proposed CABIC and bit reshuffling are less robust to transmission errors. For error resilience, one of the possible solutions is to partition the enhancement-layer frames into multiple slices as the flexible macroblock ordering (FMO) in H.264 [14]. However, penalty on coding efficiency is expected. Thus, how to provide the optimal tradeoff between coding efficiency and error resilience still leaves lots of spaces for future research activities.

## Appendix A

This appendix shows the derivation of maximum likelihood estimator for the Laplacian parameter, $\alpha_n$. To maximize (3), the $\alpha_n$ must be the root of (A1). For simplification, we have incorporated a logarithm function in (A1) to transform the exponential terms into additions/subtractions. Since logarithm function is monotonic, the root of (A1) is also the one that maximizes (3)

$$\frac{d}{d\alpha_n}\left(\ln\left(\left(\frac{1-\alpha_n}{1+\alpha_n}\right)^M \times (\alpha_n)^{\sum_{k=1}^{M}|x_{n,k}|}\right)\right) = 0. \quad \text{(A1)}$$

After taking the derivative with respect to $\alpha_n$, (A1) can be rewritten as (A2)

$$\alpha_n^2 + \left(2\mu_X^{-1}\right)\alpha_n - 1 = 0, \text{ where } \mu_X = \frac{\sum_{k=1}^{M}|x_{n,k}|}{M}. \quad \text{(A2)}$$

Since $\alpha_n$ is a real number between 0 and 1, we exclude the root that does not meet such a constraint. Equation (A3) shows the remaining solution of $\alpha_n$ that maximizes (3).

$$\alpha_n = -\mu_X^{-1} + \sqrt{\left(\mu_X^{-1}\right)^2 + 1}, \text{ where } \mu_X = \frac{\sum_{k=1}^{M}|x_{n,k}|}{M}. \quad \text{(A3)}$$

## Appendix B

This Appendix shows the detail expressions for the conditional probability and variance. Without loss of generality, we use the example of refinement bit in Fig. 4 for illustration. Eq. (B1) lists the definition of $P[X_{n,k} \in A_1^+ | X_{n,k} \in A^+]$. Since the segment $A_1^+$ in Fig. 4 is contained in the segment $A^+$, $P[X_{n,k} \in A_1^+, X_{n,k} \in A^+]$ in (B1) can be simplified as $P[X_{n,k} \in A_1^+]$. By substituting (2) into (B1), we can further obtain the formula for $P[X_{n,k} \in A_1^+ | X_{n,k} \in A^+]$

$$\begin{aligned} &P\left[X_{n,k} \in A_1^+ | X_{n,k} \in A^+\right] \\ &\quad \triangleq \frac{P\left[X_{n,k} \in A_1^+, X_{n,k} \in A^+\right]}{P[X_{n,k} \in A^+]} \\ &\quad = \frac{P\left[X_{n,k} \in A_1^+\right]}{P[X_{n,k} \in A^+]} \\ &\quad = \frac{\sum_{x_{n,k}\in A_1^+} \frac{1-\alpha_n}{1-\alpha_n} \times (\alpha_n)^{|x_{n,k}|}}{\sum_{x_{n,k}\in A^+} \frac{1-\alpha_n}{1-\alpha_n} \times (\alpha_n)^{|x_{n,k}|}}. \end{aligned} \quad \text{(B1)}$$

In addition, (B2) lists the definition of $\mathrm{Var}[X_{n,k}|X_{n,k} \in A^+]$. As shown in (B2), the calculation of conditional variance involves the conditional expectation. To compute such an intermediate result, (B3) defines the conditional $m$th moment of $X_{n,k}$ given $X_{n,k} \in A^+$

$$\begin{aligned} &\mathrm{Var}[X_{n,k}|X_{n,k} \in A^+] \\ &\quad \triangleq E\left[(X_{n,k})^2 | X_{n,k} \in A^+\right] \\ &\qquad - \left(E[X_{n,k}|X_{n,k} \in A^+]\right)^2; \end{aligned} \quad \text{(B2)}$$

$$\begin{aligned} &E\left[(X_{n,k})^m | X_{n,k} \in A^+\right] \\ &\quad \triangleq \sum (x_{n,k})^m \times P[X_{n,k} = x_{n,k} | X_{n,k} \in A^+]. \end{aligned} \quad \text{(B3)}$$

By substituting (B3) and (2) into (B2), (B4) shows the formula for the $\mathrm{Var}[X_{n,k}|X_{n,k} \in A^+]$

$$\begin{aligned} \mathrm{Var}[X_{n,k}|X_{n,k} \in A^+] = &\frac{\sum_{x_{n,k}\in A^+} (x_{n,k})^2 \times \frac{1-\alpha_n}{1-\alpha_n} \times (\alpha_n)^{|x_{n,k}|}}{\sum_{x_{n,k}\in A^+} \frac{1-\alpha_n}{1-\alpha_n} \times (\alpha_n)^{|x_{n,k}|}} \\ &- \left(\frac{\sum_{x_{n,k}\in A^+} x_{n,k} \times \frac{1-\alpha_n}{1-\alpha_n} \times (\alpha_n)^{|x_{n,k}|}}{\sum_{x_{n,k}\in A^+} \frac{1-\alpha_n}{1-\alpha_n} \times (\alpha_n)^{|x_{n,k}|}}\right)^2. \end{aligned} \quad \text{(B4)}$$

For the calculation of the other conditional probabilities and variances in (6)–(9), one simply needs to modify the ranges of summation in (B1) and (B4).

## REFERENCES


[1] Y. Chen, R. Hayder, and M. van der Schaar, "Fine Granular Scalable Video With Embedded DCT Coding of the Enhancement Layer," DN/20030133499, U.S. patent application.

[2] T. M. Cover and J. A. Thomas, *Elements of Information Theory*. New York: Wiley, 1991.

[3] H. C. Huang and T. Chiang, "Stack robust fine granularity scalability," in *Proc. IEEE Int. Symp. Circuits and Systems*, Vancouver, BC, Canada, 2004.

[4] H. C. Huang, C. N. Wang, and T. Chiang, "A robust fine granularity scalability using trellis based predictive leak," *IEEE Trans. Circuits Syst. Video Technol.*, vol. 12, no. 6, pp. 372–385, Jun. 2002.

[5] N. K. Laurance and D. M. Monro, "Embedded DCT coding with significance masking," in *Proc. IEEE Int. Conf. Acoustics, Speech, Signal Processing*, Munich, Germany, 1997.

[6] J. Li and S. Lei, "An embedded still image coder with rate-distortion optimization," *IEEE Trans. Image Process.*, vol. 9, no. 7, pp. 297–307, Jul. 2003.

[7] W. Li, "Overview of fine granularity scalability in MPEG-4 standard," *IEEE Trans. Circuits Syst. Video Technol.*, vol. 11, no. 3, pp. 301–317, Mar. 2001.

[8] D. Nister and C. Christopoulos, "An embedded DCT-based still image coding algorithm," in *Proc. IEEE Int. Conf. Acoustics, Speech, and Signal Processing*, Seattle, WA, 1998.

[9] W. H. Peng and Y. K. Chen, "Mode adaptive fine granularity scalability," in *Proc. IEEE Int. Conf. Image Processing*, Thessaloniki, Greece, 2001.

[10] W. H. Peng, T. Chiang, and H. M. Huang, "Context based binary arithmetic coding for fine granularity scalability," in *Proc. IEEE Int. Symp. Signal Processing and its Applications*, Paris, France, 2003.

[11] W. H. Peng, C. N. Wang, T. Chiang, and H. M. Hang, "Context adaptive binary arithmetic coding with stochastic bit reshuffling for advanced fine granularity scalability," in *Proc. IEEE Int. Symp. Circuits and Systems*, Vancouver, BC, Canada, 2004.

[12] J. Reichel, H. Schwarz, and M. Wien, Scalable Video Coding Working Draft 2 , ISO/IEC JTC1/SC29/WG11 and ITU-T SG16 Q.6, JVT-O201, 2005.

[13] J. M. Shaprio, "Embedded image coding using zerotrees of wavelet coefficients," *IEEE Trans. Signal Process.*, vol. 41, no. 12, pp. 3445–3462, Dec. 1993.

[14] T. Weigand, Draft ITU-T Recommendation and Final Draft International Standard of Joint Video Specification (ITU-T Rec. H.264—ISO/IEC 14496-10 AVC) , ISO/IEC JTC1/SC29/WG11 and ITU-T SG16 Q.6, JVT-G050, 2003.

[15] F. Wu, S. Li, X. Sun, B. Zeng, and Y. Q. Zhang, "Macroblock-based progressive fine granularity scalable video coding," *Int. J. Imaging Syst. Technol.*, vol. 13, no. 6, pp. 913–924, 2003.


**Wen-Hsiao Peng** was born in Hsinchu, Taiwan, R.O.C., in 1975. He received the B.S. and M.S. degrees (with highest distinction) in electronics engineering in 1997 and 1999, respectively, from National Chiao-Tung University, Hsinchu, where he is currently pursuing the Ph.D. degree at the Institute of Electronics.

In 2000, he joined Intel Microprocessor Research Laboratory, Santa Clara, CA, where he developed the first real-time MPEG-4 FGS codec and demonstrated its application in a 3-D, peer-to-peer video conferencing. Since 2004, he has actively participated in ISO's Moving Picture Expert Group (MPEG) digital video coding standardization process and contributed to the development of MPEG-4 Part 10 AVC Amd.1 scalable video coding (SVC) standard. His major research interests include scalable video coding, video codec optimization, and platform-based architecture design for video compression. He has published over 20+ technical papers in the field of video and signal processing.

**Tihao Chiang** (S'91–M'95–SM'99) was born in Chia-Yi, Taiwan, R.O.C., in 1965. He received the B.S. degree in electrical engineering from the National Taiwan University, Taipei, in 1987, the M.S. degree in electrical engineering in 1991 and the Ph.D. degree in electrical engineering in 1995, both from Columbia University, New York.

In 1995, he joined the David Sarnoff Research Center, Princeton, NJ, as a Member of Technical Staff, and was later promoted to Technology Leader and Program Manager. While at Sarnoff, he led a team of researchers and developed an optimized MPEG-2 software encoder. In September 1999, he joined the faculty at National Chiao-Tung University, Hsinchu, Taiwan. Since 1992, he has actively participated in ISO's Moving Picture Experts Group (MPEG) digital video coding standardization process with particular focus on the scalability/compatibility issue. He is currently the co-editor of Part 7 of the MPEG-4 Committee and has made more than 90 contributions to the MPEG Committee over the past ten years. His main research interests are compatible/scalable video compression, stereoscopic video coding, and motion estimation. He holds 13 U.S. patents and 30 European and worldwide patents and has published over 50 technical journal and conference papers in the field of video and signal processing.

Dr. Chiang was a co-recipient of the 2001 Best Paper Award from the IEEE TRANSACTIONS ON CIRCUITS AND SYSTEMS FOR VIDEO TECHNOLOGY. For his work in the encoder and MPEG-4 areas, he received two Sarnoff achievement awards and three Sarnoff team awards.

**Hsueh-Ming Hang** (S'79–M'80–SM'91–F'02) received the B.S. and M.S. degrees from National Chiao-Tung University (NCTU), Hsinchu, Taiwan, R.O.C., in 1978 and 1980, respectively, and the Ph.D. degree in electrical engineering from Rensselaer Polytechnic Institute, Troy, NY, in 1984.

From 1984 to 1991, he was with AT&T Bell Laboratories, Holmdel, NJ, and then joined the Electronics Engineering Department, NCTU, in December 1991. He has been actively involved in international video standards since 1984 and his current research interests include multimedia compression, image/signal processing, and multimedia communication systems. He holds eight patents (R.O.C., U.S., and Japan) and has published over 130 technical papers related to image compression, signal processing, and video codec architecture.

Dr. Hang was an Associate Editor of the IEEE TRANSACTIONS ON IMAGE PROCESSING (1992–1994) and the IEEE TRANSACTIONS ON CIRCUITS AND SYSTEMS FOR VIDEO TECHNOLOGY (1997–1999). He is co-editor and contributor of the *Handbook of Visual Communications* (published by Academic Press). He received the IEEE Third Millennium Medal and the IEEE ISCE Outstanding Service Award.

**Chen-Yi Lee** (M'01) received the B.S. degree from National Chiao-Tung University (NCTU), Hsinchu, Taiwan, R.O.C., in 1982 and the M.S. and Ph.D. degrees from Katholieke University Leuven (KUL), Leuven, Belgium, in 1986 and 1990, respectively, all in electrical engineering.

From 1986 to 1990, he was with IMEC/VSDM, working in the area of architecture synthesis for digital signal processing (DSP). In February 1991, he joined the faculty of the Electronics Engineering Department, NCTU, where he is currently a Professor and Department Chair. His research interests mainly include VLSI algorithms and architectures for high-throughput DSP applications. He is also active in various aspects of high-speed networking, system-on-chip design technology, very low-power designs, and multimedia signal processing. He served as the Director of the Chip Implementation Center (CIC), an organization for IC design promotion in Taiwan. He is now the Microelectronics Program Coordinator of the Engineering Division under the National Science Council of Taiwan.

Dr. Lee was the former IEEE Circuits and Systems Society Taipei Chapter Chair.